ACES Asian Chemical Editorial Society

doi.org/10.1002/asia.202401869

CHEMISTRY AN ASIAN JOURNAL Research Article

www.chemasianj.org

Fine-Tuning NIR-Absorbing BODIPYs for Photoacoustic Detection of Hypochlorous Ion (OCl^-)

Prosenjit Isar[+],[a] Tarushyam Mukherjee[+],[b] Tengfei Ji,[a] Alexander Nellessen,[a] Jean Michel Merkes,[a] Fabian Kiessling,[b] Magnus Rueping,[b, c] and Srinivas Banala*[a, b]

Highly reactive oxygen and nitrogen species (ROS/RNS) play crucial roles in various pathological conditions. Among them, hypochlorous ion (OCl^-), a potent ROS, is associated in numerous oxidative stress-related disorders. Elevated levels of OCl^- are thus recognized as a biomarker for diagnosing inflammatory conditions. To enable selective detection of OCl^- via photoacoustic (PA) imaging, we present development of a near infrared(NIR)-absorbing BODIPY-based acoustogenic probe. Four regioisomers of methoxyphenols-conjugated BODIPYs were synthesized to investigate the positional influence on OCl^- selectivity over other ROS/RNS. Our study reveals that only one isomer, 4-methoxy phenol conjugation, exhibited exceptional selectivity for OCl^- without any competitive reactions, making it suitable for PA imaging. This study highlights the importance of regioisomers characterization in achieving intricate selectivity among competing reactive species. The fine-tuning and development of a suitable dye now enable the optimization of physicochemical properties for *in vivo* OCl^- detection using PA imaging.

Introduction

Photoacoustic (PA) imaging is an attractive non-invasive bioimaging modality currently in clinical translation.[1] PA combines the sensitivity of optical imaging with the high penetration depth of ultrasound.[2] PA signal can be generated either from endogenous pigments such as differentially oxygenated hemoglobin[3] or melanin[4] or collagen,[5] or from exogenous agents,[6] by shining a near infrared (NIR, 680–970 nm and 1064 nm) laser light. Apart from the development of standalone exogenous probes for PA-imaging, trigger-responsive probes (also known as acoustogenic probes) have been investigated. These probes exploit changes in their environment, like in hypoxia, the presence of metal ions,[7] bioanalytes,[8] or reaction of reactive species, to produce a detectable signal.

Reactive oxygen / nitrogen species (ROS: $O_2^{\bullet -}$, $OH^{\bullet}$, OCl^-, H_2O_2 and RNS: NO, NO^-, $ONOO^-$) are of particular interest for detection,[9] as they play vital roles in both physiological, pathogenic functions.[10] As their overproduction is associated with pathological disease,[11] detecting these levels is therefore important. Advances have been made in the field with other imaging modalities, but we are particularly interested in the development of acoustogenic probes for PA imaging. Our work focuses not only on the reversible detection of ROS/RNS to distinguish pathological levels from physiological ones, but also on the selective identification of individual ROS/RNS species through the design of novel probes.[12] Development of such reactive species-specific probes holds significant biological implications, serving as valuable tools for both mechanistic studies and diagnostic applications.[13] Previously, we successfully developed probes suitable for reversible[12c] and irreversible detection of superoxide ion ($O_2^{-\bullet}$), a primary ROS.[12b] Secondary reactive species, generated from subsequent reactions of $O_2^{-\bullet}$ under biological conditions, are also implicated in the onset of various diseases, thus our efforts are directed to selectively detect other species.

Hypochlorous ion (Ocl^-) plays a crucial role in immune system reactions against infection but is also associated in chronic inflammation and in some cancers progression.[14] In neutrophils, over 70% of the H_2O_2 produced is converted to HOCl through the reaction with Cl^- ions, catalysed by the enzyme myeloperoxidase (MPO) (Figure 1). Therefore, developing effective methods and probes for the detection of Ocl^- and differentiating it from other species is essential for investigating its function and fate in living organisms.[15] To date, techniques like chromogenic, colorimetric, (chemi)luminescent, fluorescent and electrochemical have been explored by utilizing different probes that change their inherent properties upon reaction with OCl^-.[16] Since real-time, non-invasive detection of the transient OCl^- (and other ROS) is not possible by conventional

[a] Dr. P. Isar,[+] Dr. T. Ji, A. Nellessen, Dr. J. M. Merkes, Dr. S. Banala
Institute of Organic Chemistry
RWTH Aachen University
Landoltweg 1, 52074 Aachen. Germany
E-mail: srinivas.banala@oc.rwth-aachen.de

[b] Dr. T. Mukherjee,[+] Prof. Dr. F. Kiessling, Prof. Dr. M. Rueping, Dr. S. Banala
Institute for Experimental Molecular Imaging (ExMI),
University Clinic RWTH Aachen,
Forckenbeckstraße 55, 52074 Aachen, Germany
E-mail: sbanala@ukaachen.de

[c] Prof. Dr. M. Rueping
KAUST Catalysis Center (KCC)
King Abdullah University of Science and Technology (KAUST)
23955-6900 Thuwal, Saudi Arabia

[+] These authors contributed equally.

Supporting information for this article is available on the WWW under https://doi.org/10.1002/asia.202401869

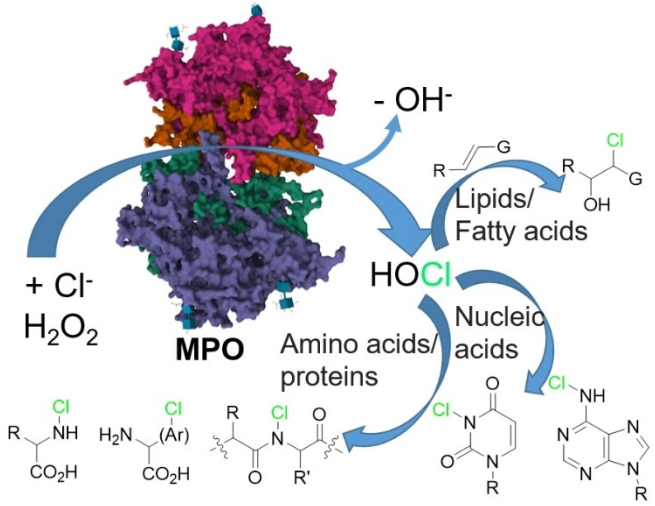

Figure 1. Schematic depiction of hypochlorous acid generation by myeloperoxidase (MPO), and its reactions with selected biomolecules.

technologies, indirect detection approaches by using acoustogenic probes could be explored. As PA is capable of real-time imaging including living animals, we aimed to develop PA-suitable, OCl^--specific activatable probes based on boron-dipyrromethene (BODIPY).

Among various chromophore classes, BODIPY dyes have been extensively studied in bio-imaging applications,[17] due to their high photostability, excellent biocompatibility,[18] and tunability into NIR range via conjugation extension.[19] Building on our previous success with a reversible $O_2^{-\bullet}$-selective BODIPY probe [ROS BODIPY **2**],[12c] we have now focused on the selective detection of OCl^-. In this work, we report the design and synthesis of conjugation-extended BODIPY dyes, their photophysical properties, reactions with different ROS, and 'turn on' acoustogenicity in particular to OCl^- induced gain in PA-signal.

Results and Discussion

The design principle leverages the strong oxidative characteristics of OCl^- by attaching redox-active synthons to reporter probes, in line with other detection techniques. Among various reported synthons, (methoxy)phenol (methoxyhydroquinone) was found to be particularly suitable for PA applications, as OCl^- oxidizes it to form a quinone.[20] To establish a structure-property relationship, we planned to conjugate three isomeric methoxyphenols to determine the effect of position, and evaluate the electronic effects using a chlorine-substituted methoxyphenol, as well as a chlorophenol lacking methoxy group. (Scheme 1)

To conjugate methoxyphenols to BODIPY, we selected the 3′,5′-positions, resulting in conjugation-extended BODIPYs expected to exhibit absorption in the NIR-region.[21] These BODIPYs show high fluorescence emission (Figure 2B), thus expected to give a weak PA signal as previously demonstrated.[22] The reaction of OCl^- is expected to produce quinone-conjugated BODIPY *in situ*, leading to quencher-type

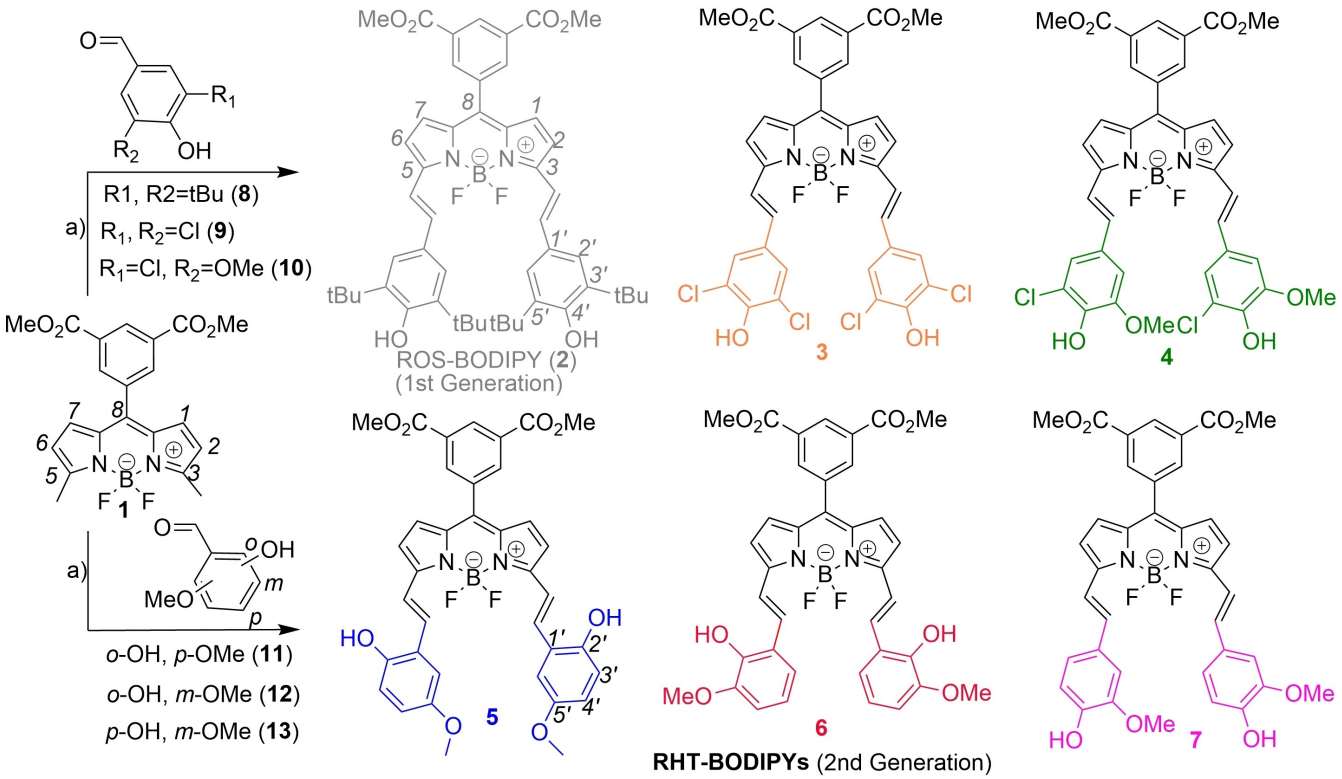

Scheme 1. Synthetic route to conjugation extended-RHT-BODIPYs: a). 2.1 eq. of aldehyde, piperidine, CH_3CO_2H, toluene, 140 °C (azeotropic distillation).

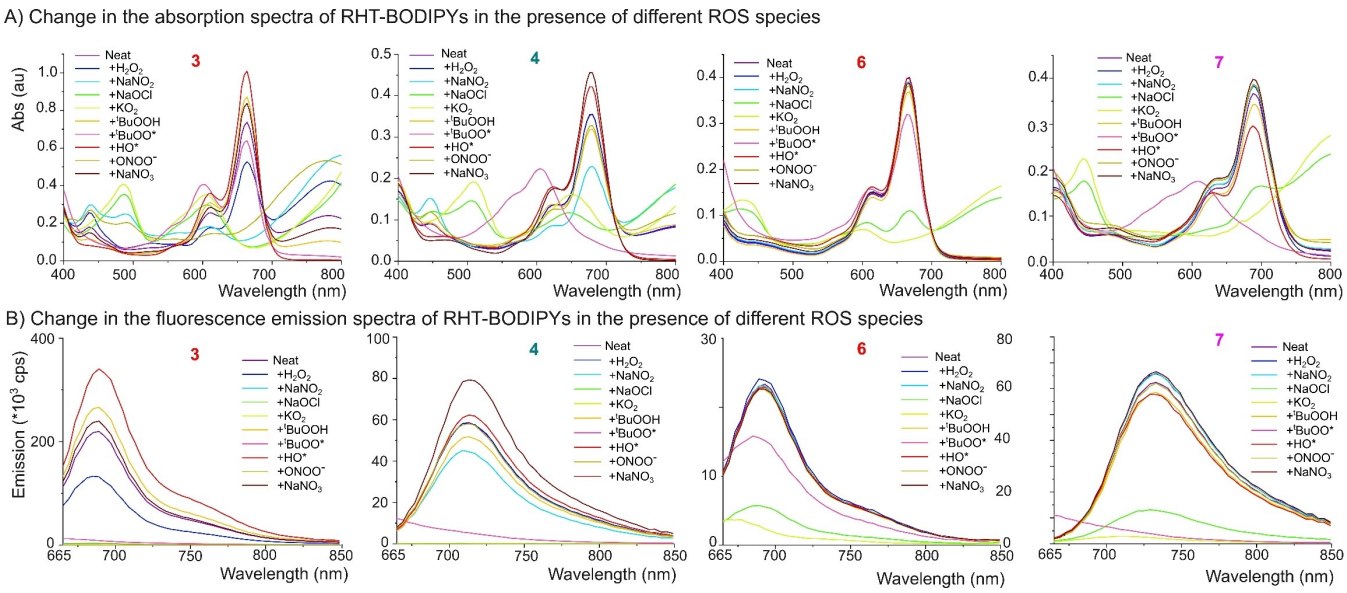

Figure 2. The absorption spectra (top panel A), and emission spectra for excitation at 635 nm (panel B) of RHT-BODIPYs (**3,4,6,7**), both in their neat form and after addition of excess ROS/RNS species (Abs: 10 μM in DMSO; Emt: 2.5 μM);

dyes with altered optical properties, which also affect their PA characteristics. This makes the conjugation of methoxyphenol to BOIDPY highly suitable for OCl^- detection.

Previously established Knoevenagel chemistry for compound **2** was applied for the conjugation of methoxyphenols using appropriate aldehyde (Scheme 1). A slight modification was introduced in synthetic procedure, replacing methane sulfonic acid with acetic acid, under azeotropic distillation piperidine contained toluene. The reaction of BODIPY **1** with different (hydroxy,methoxy)-arylaldehydes (**10**-**13**) thus produced conjugation-extended dyes **4**–**7** (RHT-BODIPYs). Also, a conjugated-BODIPY (**3**) lacking a methoxy group was prepared from **1** using 3,5-dichloro-4-hydroxybenzaldehyde (**9**) (see *Electronic Suppl. Info.*, ESI).

The absorption of dyes **3**–**7** (in DMSO solution) exhibited maxima in the range of 665 to 690 nm (Table 1; Figure 2). The (*meta*-methoxy) *para*-hydroxy aryl conjugation in dyes **4** and **7**, showed redshifted absorption, while the (*meta*-methoxy) *ortho*-hydroxy in dye **6** displayed a blue-shifted absorption. The *para*-hydroxy (3,5-dichloro−)phenyl substituted **3** also exhibited a blue-shifted maximum. Dyes **5** and **6**, either *meta*-methoxy or *para*-methoxy substitutions, showed very similar absorption maxima.

Table 1. The optical data of RHT-BODIPYs in neat, and with ROS triggers.[a]

Conj. BODIPY	Abs_{Max} (neat), nm	Emt_{Max}[b] (neat), nm	PA_{Max}[c] with OCl^-	Competing ROS[c]
2	688	723	820	Broad
3	664	689	825	Broad
4	680	713	880	Broad
5	673	697	850	**none**
6	668	693	825	$O_2^{\bullet-}$
7	692	733	820	$O_2^{\bullet-}$

[a] In DMSO; [b] Exc. at 635 nm; [c] freshly ROS-treated solutions

After the characterization, we studied the dyes' **3–7** reactions with different ROS and RNS species ($O_2^{\bullet-}$, OCl^-, $OH^{\bullet}$, $^tBuO^{\bullet}$, H_2O_2, ^tBuOOH, $ONOO^-$, NO_2^-, and NO_3^-) in DMSO solutions. The 3,5-chlorinated-4-hydroxy phenyl conjugated **3** exhibited highly sensitive and broad spectrum detection of ROS/RNS (see Figure 2 top left), showing a reactivity that was very similar to the previously described 3,5-di-^{tert}−butylphenol-conjugated **2** (for optical and PA spectra of **2**, see Figures S1, S2 and S3 in ESI),[12c] except with tBuOOH, where the **3** did not react. Similarly, the BODIPY **4** exhibited broad spectrum reactivity with ROS/RNS, in contrast to the selectivity observed with BODIPY **7** lacking a chlorine. This suggests that the presence of an extra chlorine on (3-methoxy)-4-hydroxy phenyl group negatively impacts ROS selectivity. The ROS/RNS reactions with two BODIPY isomers, **6** and **7**, revealed that both exhibited high selectivity towards OCl^-, resulting a significant redshift in absorption of over $>$120 nm. However, a competing reaction with $O_2^{\bullet-}$ was also observed, while no other ROS/RNS affected their optical properties (Figure 2B).

The best selectivity for OCl^- was observed with RHT-BODIPY **5**, which exhibited an impressive redshift of 175 nm, and showed no competing reaction with other ROS/RNS (Figure 3A). In contrast with other dyes, the competing reaction of $O_2^{\bullet-}$ led decomposition of dye **5**, (see Figure S4, ESI) making **5** exclusively sensitive to OCl^-. Surprisingly, the $^tBuO^{\bullet}$ induced a blueshift in absorption spectrum of **5**, similar to the observation in compounds **4**, **7**.

After characterizing the optical response of BODIPYs **3–7** towards ROS/RNS, we evaluated their PA spectroscopic characteristics, as summarized in Figure 4. Similar to the changes observed in their absorption spectra with different ROS/RNS,

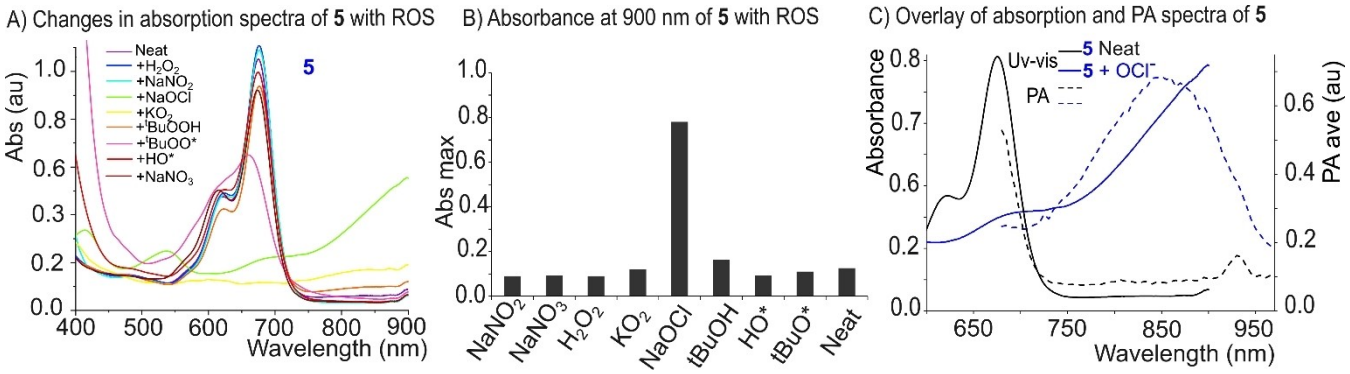

Figure 3. A) Absorption spectra of RHT-BODIPY (**5**) towards different ROS/RNS species (20 μM, in DMSO). B) The ROS/RNS-induced change in the absorption signal at 900 nm, and C) Absorption and PA-spectral overlay OCl^- selective dye **5**.

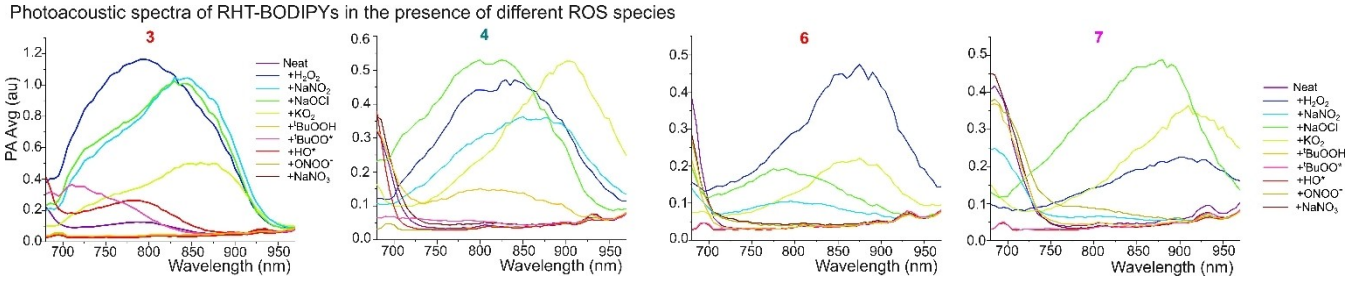

Figure 4. PA spectra of four RHT-BODIPY dyes, both in their neat and after ROS/RNS-reaction (25 μM in DMSO).

corresponding shifts in PA spectra were clearly detected. These changes included a significant increase in PA signal intensity, and an average redshift of the maxima by over 150 nm. To quantify the ROS-induced enhancement, the PA gain ratio at 875 nm was calculated relative to the PA signal of neat dye at 875 nm (Figure 5). Among the tested, broad ROS/RNS-reactive dye **3** clearly surpassed the rest, exhibiting the highest gain ratio, exceeding a tenfold increase. The dye **4** also reacted with most of ROS/RNS, PA characteristics are comparable to that of **3**, but except highest redshift with $O_2^{\bullet-}$. The isomeric dyes **6**, **7** are also sensitive to H_2O_2, and $O_2^{\bullet-}$ along with OCl^-, notably **7** showed a change in the PA maxima in reaction with OCl^- over

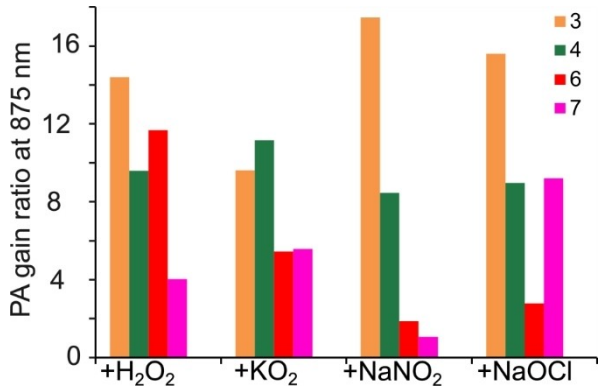

Figure 5. ROS-induced gain of the PA signal at 875 nm, compared to the neat dye, expressed as the ratio of PA Average at 875 nm (25 μM in DMSO) of four RHT-BODIPY dyes.

$O_2^{\bullet-}$ or H_2O_2, thus enabling selective detection of OCl^- via spectral characteristics.

The most OCl^--selective BODIPY, compound **5**, was further characterized using photoacoustic spectroscopy. The absorption and PA spectral overlay confirmed that BODIPY **5** exhibited good overlap in its neat dye (Figure 3C). However, upon reaction with OCl^-, the overlap became less precise – an effect observed with BODIPY dyes. Nevertheless, due to the high selectivity with a 9-fold signal enhancement, accompanied by 175 nm redshift compared to the neat dye, **5** is a promising probe for OCl^- detection.

To identify the PA active species generated by OCl^-, dyes **4**, **7** were titrated in NMR by adding an aqueous NaOCl solution. As the amount of OCl^- increased, a clear loss of the signal at 4 ppm, belonging to methoxy group, was observed (Figures S15-S20). The remaining peaks associated to the rest of the dye molecules were still identifiable, though with a poor resolution, indicating aggregation of the formed product. This observation aligns with the previously reported reactions of OCl^- at methoxy group, leading to the formation of gaseous CH_3Cl and formation of phenol (catechol).

Conclusions

In conclusion, we here present the design and synthesis of RHT-BODIPYs (**3**-**7**), combined with detailed optical characterization with ROS and RNS. By varying the positions of identical substituents, and using PA spectral characteristics to distinguish

competing species, selective detection of hypochlorous ion (OCl^-) was achieved. Among the isomeric compounds **5–7**, containing identical functional groups, the observed differences in reactivity highlights the importance of fine-tuning not only the specific groups, but also their positions to achieve selectivity. Our findings also confirm that, even in the presence of competing reactivity among regioisomers, the changes in PA spectra are characteristic for specific ROS in dyes, allowing for the differentiation of individual ROS/RNS. From this optimization and selection of the most suitable OCl^--responsive isomer, BODIPY **5**, the next steps will involve modifying its physicochemical properties for *in vivo* application. To achieve this, incorporating long PEG-arms at the *meso*-position of the BODIPY core, without compromising its reactivity to ROS, represents a promising approach. Our ongoing and future studies will build upon this strategy for acoustogenic *in vivo* detection of hypochlorous ion.

Acknowledgements

Financial support from the Central Innovation for SMEs (ZIM) initiative of the German federal government (BMWK) is gratefully acknowledged. Open Access funding enabled and organized by Projekt DEAL.

Conflict of Interests

The authors declare no conflict of interest.

Data Availability Statement

The data that support the findings of this study are available in the supplementary material of this article.

Keywords: Photoacoustic imaging · conjugated BODIPYs · reactive oxygen species · hypochlorous ion detection · NIR-imaging probes

[1] a) I. Steinberg, D. M. Huland, O. Vermesh, H. E. Frostig, W. S. Tummers, S. S. Gambhir, *Photoacoustics* **2019**, *14*, 77–98; b) H. Liu, M. Wang, F. Ji, Y. Jiang, M. Yang, *J. Biomed. Opt.* **2024**, *29*, S11522; c) Z. Wang, F. Yang, W. Zhang, K. Xiong, S. Yang, *Fundam. Res.* **2024**, *4*, 1314–1330.
[2] a) L. V. Wang, *Photoacoustic Imaging and Spectroscopy*, CRC Press, Boca Raton, FL, **2009**; b) L. V. Wang, S. Hu, *Science* **2012**, *335*, 1458–1462; c) C. Li, L. V. Wang, *Phys. Med. Biol.* **2009**, *54*, R59–R97; d) S. Zackrisson, S. M. W. Y. van de Ven, S. S. Gambhir, *Cancer Res.* **2014**, *74*, 979–1004.
[3] M. Gerling, Y. Zhao, S. Nania, J. K. Norberg, C. S. Verbeke, B. Englert, R. V. Kuiper, Å. Bergström, M. Hassan, A. Neesse, J. M. Löhr, R. L. Heuchel, *Theranostics* **2014**, *4*, 604–613.
[4] I. Stoffels, S. Morscher, I. Helfrich, U. Hillen, J. Leyh, N. C. Burton, T. C. P. Sardella, J. Claussen, T. D. Poeppel, H. S. Bachmann, A. Roesch, K. Griewank, D. Schadendorf, M. Gunzer, J. Klode, *Sci. Transl. Med.* **2015**, *7*, 317ra199.
[5] A. P. Regensburger, L. M. Fonteyne, J. Jüngert, A. L. Wagner, T. Gerhalter, A. M. Nagel, R. Heiss, F. Flenkenthaler, M. Qurashi, M. F. Neurath, N. Klymiuk, E. Kemter, T. Fröhlich, M. Uder, J. Woelfle, W. Rascher, R. Trollmann, E. Wolf, M. J. Waldner, F. Knieling, *Nat. Med.* **2019**, *25*, 1905–1915.
[6] a) Q. Fu, R. Zhu, J. Song, H. Yang, X. Chen, *Adv. Mater.* **2019**, *31*, 1805875; b) P. K. Upputuri, M. Pramanik, *J. Biomed. Opt.* **2019**, *24*, 040901.
[7] L. Zeng, G. Ma, H. Xu, J. Mu, F. Li, X. Gao, Z. Deng, J. Qu, P. Huang, J. Lin, *Small* **2019**, *15*, 1803866.
[8] C. J. Reinhardt, R. Xu, J. Chan, *Chem. Sci.* **2020**, *11*, 1587–1592.
[9] X. Chen, F. Wang, J. Y. Hyun, T. Wei, J. Qiang, X. Ren, I. Shin, J. Yoon, *Chemical Society Reviews* **2016**, *45*, 2976–3016.
[10] a) G. Maulucci, G. Bačić, L. Bridal, H. H. H. W. Schmidt, B. Tavitian, T. Viel, H. Utsumi, A. S. Yalçin, M. De Spirito, *Antiox. Redox Signal.* **2016**, *24*, 939–958; b) O. S. Kornfeld, S. Hwang, M. H. Disatnik, C. H. Chen, N. Qvit, D. Mochly-Rosen, *Circulation Research* **2015**, *116*, 1783–1799.
[11] C. H. Liu, N. D. Abrams, D. M. Carrick, P. Chander, J. Dwyer, M. R. J. Hamlet, A. L. Kindzelski, M. PrabhuDas, S. Y. A. Tsai, M. M. Vedamony, C. Wang, P. Tandon, *FASEB Journal* **2019**, *33*, 13085–13097.
[12] a) M. Jean Michel, K. Fabian, B. Srinivas, *Curr. Med. Chem.* **2022**, *29*, 6008–6029; b) J. M. Merkes, M. Rueping, F. Kiessling, S. Banala, *ACS Sensors* **2019**, *4*, 2001–2008; c) J. M. Merkes, A. Hasenbach, F. Kiessling, S. Hermann, S. Banala, *ACS Sensors* **2021**, *6*, 4379–4388.
[13] a) A. C. Stiel, V. Ntziachristos, *Nature Methods* **2024**, *21*, 1996–2007; b) B. Kalyanaraman, V. Darley-Usmar, K. J. A. Davies, P. A. Dennery, H. J. Forman, M. B. Grisham, G. E. Mann, K. Moore, L. J. Roberts, H. Ischiropoulos, *Free Radic. Biol. Med.* **2012**, *52*, 1–6.
[14] C. M. C. Andrés, J. M. Pérez de la Lastra, C. A. Juan, F. J. Plou, E. Pérez-Lebeña, *Int. J. Mol. Sci.* **2022**, *23*, 10735.
[15] Y. C. Yang, H. H. Lu, W. T. Wang, I. Liau, *Anal. Chem.* **2011**, *83*, 8267–8272.
[16] a) R. Zhang, B. Song, J. Yuan, *TrAC Trends Anal. Chem.* **2018**, *99*, 1–33; b) Y. Yue, F. Huo, C. Yin, J. O. Escobedo, R. M. Strongin, *Analyst* **2016**, *141*, 1859–1873.
[17] E. Antina, N. Bumagina, Y. Marfin, G. Guseva, L. Nikitina, D. Sbytov, F. Telegin, *Molecules* **2022**, *27*, 1396.
[18] A. M. Durantini, D. A. Heredia, J. E. Durantini, E. N. Durantini, *Eur. J. Med. Chem.* **2018**, *144*, 651–661.
[19] D. Pinjari, Y. Patil, R. Misra, *Chem. Asian J.* **2024**, *19*, e202400167.
[20] a) Z.-N. Sun, F.-Q. Liu, Y. Chen, P. K. H. Tam, D. Yang, *Org. Lett.* **2008**, *10*, 2171–2174; b) J. J. Hu, N.-K. Wong, Q. Gu, X. Bai, S. Ye, D. Yang, *Org. Lett.* **2014**, *16*, 3544–3547.
[21] J. M. Merkes, T. Lammers, R. Kancherla, M. Rueping, F. Kiessling, S. Banala, *Adv. Opt. Mater.* **2020**, *8*, 1902115.
[22] M. Frenette, M. Hatamimoslehabadi, S. Bellinger-Buckley, S. Laoui, J. La, S. Bag, S. Mallidi, T. Hasan, B. Bouma, C. Yelleswarapu, J. Rochford, *J. Am. Chem. Soc.* **2014**, *136*, 15853–15856.

Manuscript received: December 16, 2024
Revised manuscript received: January 29, 2025
Accepted manuscript online: January 29, 2025
Version of record online: February 14, 2025